Indian Journal of Experimental Biology
Vol. 64, November 2026, pp. 1029-1039
DOI: 10.56042/ijeb.v64i11.26558

A kaempferol-loaded dehydrated amniotic membrane scaffold for enhancing bone defect repair in rats

Zhuo Wu[1], Xiongxun Wang[1], Ruijian Peng[1] & Yingjie Zhu[1]*

[1]Xi'an International Medical Center Hospital Spine Surgery, Xi'an 710 000, Shaanxi, China

Received 17 December 2025; revised 17June 2026

Regenerative medicine has emerged as a strategic solution for managing critical-size bone defects. This study evaluated the effectiveness of a dehydrated human amniotic membrane (HAM) scaffold loaded with kaempferol in enhancing bone regeneration in rat tibial defects. Forty male Sprague–Dawley rats underwent bilateral tibial defect surgery and were assigned to four groups: untreated defects (control), kaempferol (Kaem) alone, HAM alone and HAM combined with Kaem. Bone regeneration was assessed using radiographic and histopathological analyses at 4 and 8 weeks post-surgery. The expression levels of osteogenic markers, including COL1A1, Wnt3a, β-catenin, Runx2, Osteopontin, and Osterix, were analyzed by RT-PCR. Radiographic evaluation demonstrated significantly higher scores in the HAM + Kaem group at both 4 and 8 weeks compared to controls ($P<$ 0.05). Histopathological analysis revealed a significant improvement in total bone healing scores at week 8 in the HAM + Kaem group. No significant differences were observed in inflammatory cell infiltration among groups at either time point. Gene expression analysis showed significant upregulation of all assessed osteogenic markers in the HAM + Kaem group at both time points ($P<$ 0.05). Kaem-loaded HAM enhances bone defect repair; however, further optimization is required to improve kaempferol bioavailability and therapeutic efficacy.

Keywords: Bone Defect, Human amniotic membrane, Kaempferol, Regenerative medicine, Tissue engineering

Bone injuries are one of the primary factors contributing to disability in both humans and animals across various regions of the world. Despite the inherent ability of the bone to regenerate and repair minor injuries without forming fibrotic tissue, larger defects exceeding critical size cannot be independently healed. Statistics indicate that millions of individuals worldwide suffer from bone disorders, leading to various physical and functional disabilities[1-3]. In the United States and Europe, approximately half a million patients seek medical treatment annually for bone repair. Consequently, there is a growing market demand for developing and enhancing innovative and effective regenerative methods. Indeed, the reinforcement and acceleration of bone regeneration have emerged as new objectives for orthopedic approaches to address this challenging needs[4-8].

Human amniotic membrane (HAM), which is the inner layer of the fetal membrane in contact with amniotic fluid, possesses non-tumorigenic, anti-inflammatory, and immunomodulatory properties. This membrane contains numerous essential elements, growth factors, and active biological mediators, including fibronectin, laminin, proteoglycans, elastin, collagen, hyaluronic acid, epidermal growth factor, fibroblast growth factor, and transforming growth factor[9-11]. It is believed that these compounds within the amniotic membrane exert paracrine effects that protect the damaged tissue from external factors, optimize the microenvironment, and stimulate tissue repair[9,11]. The amniotic membrane has been utilized in corneal defect reconstruction, tendon and nerve tear repair, treatment of diabetic wounds and burns, as well as prevention of adhesions post-surgery[12-18].

Kaempferol (Kaem) is a natural flavonoid extracted from the rhizome of the plant *Kaempferia galangal* L. and is also found as a natural flavonol in various medicinal plants, Chinese beans, and fruits[19,20]. Kaem exhibits anti-inflammatory[21], anti-tumorigenic[22], anti-diabetic[23], and anti-osteoporotic properties[24]. Some of Kaem's pharmacological characteristics are directly related to its bone-protective effects. Numerous studies indicate that Kaem not only has beneficial properties for cardiovascular and neurological health but also possesses anti-cancer properties and

*Correspondence:
E-mail: 28789985zhuyjbb@sina.com

prevents osteoporosis by improving bone formation and stimulating osteoblast differentiation[25,26]. Additionally, several studies have evaluated the healing effects of amniotic fluid and amniotic membrane on fractures[4,16]. Therefore, based on the findings regarding the high potential of amniotic membranes and Kaem in healing bone injuries, as well as the lack of studies investigating the combined effects of amniotic membranes and Kaem, we aimed to conduct a comprehensive quantitative study utilizing radiological, histopathological, and molecular techniques on the tibia bone tissue in rat models of bone defects. The present study describes a new bioactive scaffold strategy utilizing a naturally derived osteogenic compound integrated into a biologically active amniotic membrane matrix to enhance the local regenerative microenvironment. Moreover, unlike previous studies that focused primarily on morphological outcomes, the present work provides a comprehensive evaluation of bone regeneration through radiographic, histopathological, and osteogenic gene expression analyses.

Materials and Methods

This study is an experimental interventional animal study. All animal procedures were conducted in accordance with the ARRIVE guidelines and were approved by the Medical Ethics Committee of Xi'an International Medical Center Hospital (ID: GJYX-KY-2024-042). The donated placenta used for the production of HAM was obtained under sterile conditions from a mother with a normal pregnancy at term, following a scheduled cesarean section. The donor had negative test results for Hepatitis B, Hepatitis C, HIV, and Syphilis. The placenta was transported to the laboratory under sterile conditions at a temperature of 4°C, where the amniotic membrane was separated from the surrounding excess tissues in a completely sterile environment beneath a Class II laminar flow hood. It was then washed with Medium 199 (Sigma-Aldrich, USA) and a combination of antibiotics, including Streptomycin, Amphotericin B, and Penicillin G to ensure complete removal of blood clots and residual tissues. The amniotic membrane was subsequently placed in isotonic PBS for 24 h. Finally, to dehydrate the tissue, we utilized a freeze-dryer (model LYO60B-1PT from Bioevopeak, China). Additionally, a dosage of 10 mg of Kaem[27] was administered topically to each rat.

Experimental design

The subjects of this study included 20 adult male Sprague-Dawley rats. The animal room maintained a temperature range of approximately 20 to 22°C, with a light/dark cycle of 12 h each and relative humidity between 40% and 60%. The rats were housed in polycarbonate cages with stainless steel mesh tops, and their bedding consisted of sterilized wood shavings.

Method for inducing bone defects

Bone defects were created on both tibiae of the rats (totaling 80 bone defects). Initially, the rats were anesthetized *via* intraperitoneal injection of Ketamine/Xylazine (10/100 mg/kg) (manufactured by Alfasan, Netherlands). The surgical site was then shaved and disinfected with Betadine. In each rat, a hole measuring 2×2×7 mM was created on the tibia bone using an angle bur (carbide-tipped handpiece) with a diameter of 2 mM. The remaining bone fragments at the surgical site were washed with physiological saline. The amniotic membrane loaded with Kaem was placed into the created cavity in each group. Finally, the muscle layer was sutured using 0-5 Vicryl sutures, and the skin was closed using 0-4 nylon sutures in a subcuticular manner. After the surgery, 10 mL of normal saline was injected subcutaneously. For analgesia, Buprenorphine at a dose of 0.1 mg/kg was administered subcutaneously every 24 h for three days. Additionally, to prevent infection, Oxytetracycline powder was provided in the drinking water of the rats every other day for five days.

Grouping of Animals

The animals were randomly assigned to the four experimental groups using a computer-generated randomization method.

1. Negative control group with tibia defects (no treatment)
2. Tibia defect group + HAM
3. Tibia defect group + Kaem, and
4. Tibia defect group + HAM + Kaem.

The treatment duration for the animals was set for 4 and 8 weeks post-surgery. Ultimately, the rats underwent anesthesia at the specified intervals for radiological assessment, and after this procedure, they were euthanized for histopathological examination. Their tibiae were fixed in 10% formalin buffer. Euthanasia was performed using a CO2 chamber.

Radiological assessments

After 4 and 8 weeks post-implantation of the scaffolds, the rats were anesthetized for radiological evaluation. Radiographic assessments were conducted on the tibia region in both Anterior-Posterior and Lateral views. All images were obtained by a single operator using the Axiom Multix M Radiographic Unit (Siemens™, Germany) and following standard procedures (55 kV, 0.3 mA, and a duration of 3 seconds). Scoring was performed by a radiologist in a blinded manner, utilizing a radiological scoring table specifically designed for the rat model, based on the grading system outlined in (Table 1)[28].

Table 1 — Modified Lane and Sandhu radiological scoring system

Parameter	Value	score
Bone formation	No evidence of bone formation	0
	Bone formation occupying 25% of defect	1
	Bone formation occupying 50% of defect	2
	Bone formation occupying 75% of defect	3
Union (proximal and distal evaluated separately)	Nonunion	0
	Possible union	1
	Radiographic union	2
Remodeling	No evidence of remodeling	0
	Remodeling of medullary canal	1
	Full remodeling of cortex	2
Total point possible per category	Bone formation	4
	Proximal union	2
	Distal union	2
	Remodeling	2
Maximum score		10

RNA isolation and Gene expression analysis *via* quantitative RT-PCR (Wnt, β-catenin, Runx2, Osteopontin, Osterix)

Following euthanasia, the rat tibia bones were immediately preserved in RNA-stabilizing solution for 24 h and stored at -80°C until processing. Total RNA was extracted using Kiyanzol Isolation Reagent (QIAGEN, Venlo, Netherlands), adhering strictly to the manufacturer's protocol. For cDNA synthesis, 1 µg of purified RNA was reverse-transcribed in a 20 µL reaction volume using the QuantiTect Reverse Transcription Kit (Fermentas, USA). The resulting cDNA was stored at -20°^{C} for subsequent quantitative real-time PCR (RT-qPCR) analysis. Gene expression levels of Wnt, Runx2, Osteopontin, and Osterix in the tibial tissue were quantified using the ABI 7500 Real-Time PCR System (Applied Biosystems, USA). Primer sequences are detailed in (Table 2). Amplification specificity was confirmed *via* melt curve analysis, and reaction efficiency was validated through standard curve slopes. Relative mRNA expression was calculated using the $2^{-\Delta\Delta Ct}$ method, with GAPDH serving as the endogenous control for normalization.

Histopathological Study

Following the fixation of the tibia bones in 10% formalin buffer, a demineralization process was carried out using 10% formic acid. Subsequently, tissue processing involved fixating, dehydrating, clearing, infiltrating, and embedding in paraffin. Paraffin blocks containing bone samples were sectioned at a thickness of 5 micrometers and stained with Hematoxylin-Eosin. All slides were evaluated in

Table 2 — The sequence of designed primers

Gene Description	Accession No	Sequences (5′ - >3′)	Product size
COL1A1: Sense	NM_053304.1	AAGGCAATGCTGAATCGTCC	153
COL1A1: Anti-sense		TGTGTGGGGATTTGTTGCAG	
Osterix: Sense	NM_181374.2	TCAAGCACCAATGGACTCCT	168 bp
Osterix: Anti-sense		GCCATAGTGAGGCTTCTTCC	
Osteopontin: Sense	NM_012881.2	CTTGGCTTACGGACTGAG	136 bp
Osteopontin: Anti-sense		AACTGGGATGACCTTGATAG	
Runx2: Sense	NM_001278483.2	TGTGTGCCTCCAACCTGTGT	71 bp
Runx2: Anti-sense		CTTTCCCCCTCAATTTGTGTC	
β-catenin: Sense	NM_001098209	CATCACCACGCTGCATAATC	100bp
β-catenin: Anti-sense		GAGCTTGCTTTCCTGATTGC	
Wnt3a: Sense	NM_001414349.1	TCTGCCATGAACCGTCACAA	115 bp
Wnt3a: Anti-sense		ACCAGCAGGTCTTCACTTCG	
GAPDH : Sense	NM_017008.4	CAGCAAGGATACTGAGAG CAA GAG	100 bp
GAPDH: Anti-sense		GGATGGAATTGTGAGGGAGATG	

COL1A1 collagen type I alpha 1, RUNX2 runt-related transcription factor 2, GAPDH glyceraldehyde phosphate dehydrogenase, Wnt3a Wingless-type MMTV Integration Site Family, Member 3A. Kaem: Kaempferol, HAM: human amniotic membrane, COL1A1: Collagen Type I Alpha 1 Chain, Wnt3a: Wnt Family Member 3A, Runx2: Runt-Related Transcription Factor 2

Table 3 – Dual-category histopathological evaluation framework for assessing fracture repair and associated tissue reactions

Categories	Parameters	score				
		3	2	1	0	
Fracture healing	Callus formation	Full-across the defect	Moderate (>50%)	Mild (<50%)	None	
	Bone union	Full bone bridge union	Moderate (>50%)	Mild (<50%)	No new bone in the fracture line-nonunion	
	Marrow changes	Adult type fatty marrow	> 50% replaced by new tissue	< 50% replaced by new tissue	Fibrous tissue or red	
	Cortex remodeling	Full remodeling cortex	Moderate remodeling >50%	Mild remodeling <50%	No remodeling	
	Parameters	4	3	2	1	0
Tissue response	Fibrous connective tissue formation	Severe deposition of dense collagen connective tissue around implant	Disruption of normal tissue architecture and presence of moderately dense fibrous connective tissue	Presence of moderate connective tissue	Presence of delicate spindle shaped cells or mild fibroplasia	No difference from normal control tissue, no presence of connective tissue at or around implant site
	Inflammatory cellular infiltration	Severe cellular infiltrate response to implant or tissue necrosis at or around the site	Presence of large numbers of lymphocytes, macrophages and foreign body giant cells, also notable presence of eosinophils and neutrophils	Presence of several lymphocytes, macrophages with a few foreign body giant cells and a small focus of neutrophils	Presence of a few lymphocytes or macrophages, no presence of foreign body giant cells, eosinophils, or neutrophils	No difference from normal control tissue, no presence of macrophages, foreign body cells, lymphocytes, eosinophils, or neutrophils at or around implant site

(Kaem: Kaempferol, HAM: human amniotic membrane, COL1A1: Collagen Type I Alpha 1 Chain, Wnt3a: Wnt Family Member 3A, Runx2: Runt-Related Transcription Factor 2)

a blinded manner by a pathologist according to the scoring table presented in (Table 3)[29], using a Nikon E200 optical microscope.

Statistical Analysis

Data analysis was performed using IBM SPSS statistical software (version 23; SPSS Inc., Chicago, Illinois, USA). Initially, the distribution of variables was assessed using the Kolmogorov-Smirnov test. For the statistical analysis of histopathological and radiological data, descriptive statistics, including mean, standard deviation, and the minimum and maximum values of the median, were calculated using the Kruskal-Wallis test. Additionally, one-way ANOVA and post hoc Tukey tests were employed to evaluate the gene expression levels, with corresponding histograms generated using GraphPad software (version 6.07).

Results

Results related to radiological evaluation

The results of the radiological assessments conducted in the fourth week indicated a significant increase in the radiological score in the Kaem (Kaem) and HAM + Kaem groups compared to the control group (P = 0.042 and P = 0.001, respectively) (Fig 1a). In the eighth week, the radiological score in the HAM + Kaem group demonstrated a significant increase compared to both the HAM group (P= 0.034) and the control group (P=0.001) (Fig 1b). No significant differences were observed among the other groups (Fig 1a & b), (Fig 2a-i).

mRNA Gene expression of COL1A1, Osterix, Osteopontin, Runx2, β-catenin, and Wnt3a

The expression level of the COL1A1 gene in the Kaem and HAM + Kaem groups showed a significant increase at both the fourth and eighth weeks compared to the control and HAM groups (P< 0.05) (Fig 3a & b). In the fourth week, the expression level of the Osterix gene in the HAM + Kaem group significantly increased compared to the control group (P=0.013) (Fig 3c). By the eighth week, the expression levels of the Osterix gene in the Kaem and HAM + Kaem groups also exhibited significant increases compared to the control group, with p-values of 0.019 and 0.009, respectively (Fig 3d).

The expression level of the Osteopontin gene in the Kaem and HAM + Kaem groups showed a significant increase at the fourth week compared to both the

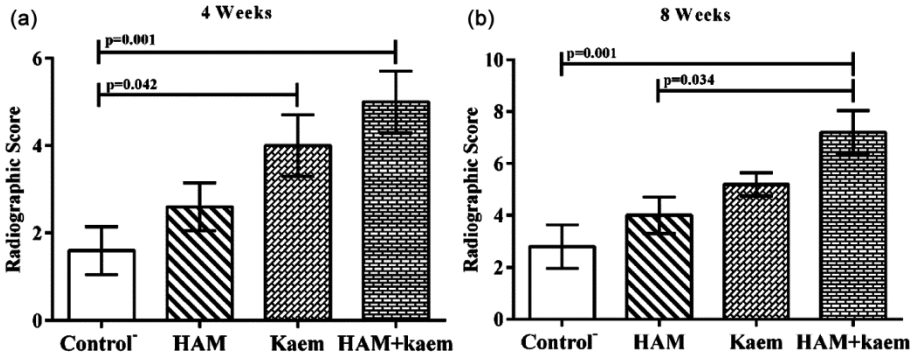


Fig. 1 — Results of radiographic assessments at weeks 4 (a) and 8 (b) after the initiation of the experiment. Each value is shown as Mean ± SD. The Kruskal-Wallis test was used for analysis. $P< 0.05$ was considered statistically significant. Kaem: Kaempferol, HAM: human amniotic membrane

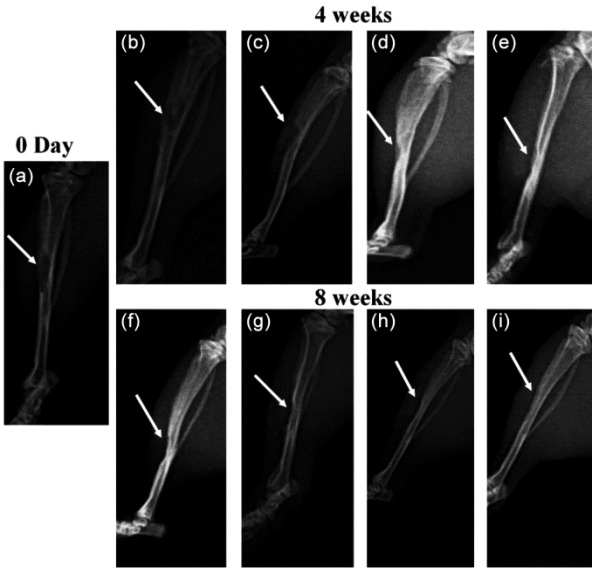


Fig. 2 — Radiographic images in different groups, immediately after surgery, and at the fourth and eighth weeks after surgery. The rats are separated into four groups: Control⁻ (A & F), HAM (B &G), Kaem (C & H), and HAM + Kaem (D & I). The arrow indicates the location of the defects. Kaem: Kaempferol, HAM: human amniotic membrane

control and HAM groups ($P< 0.05$) (Fig 3e). In the eighth week, the expression levels of the Osteopontin gene in the Kaem and HAM + Kaem groups also demonstrated significant increases compared to the control group ($P = 0.025$ and $P = 0.004$, respectively) (Fig 3f). Furthermore, the expression level of Osteopontin in the HAM + Kaem group significantly increased compared to the HAM group at week eight (P=0.001) (Fig 3f).

The results indicated a significant increase in the expression levels of the Runx2 and Wnt3a genes in the HAM + Kaem group at week 4 compared to the control and HAM groups ($P< 0.05$) (Fig 3g & k). Additionally, the expression levels of Runx2 and Wnt3a genes at week 8 also demonstrated a significant increase in the Kaem and HAM + Kaem groups compared to the control and HAM groups ($P< 0.05$) (Fig 3 h & l). The expression level of the β-catenin gene showed a significant increase in both the Kaem and HAM + Kaem groups at weeks 4 and 8 compared to the control group ($P< 0.05$) (Fig 3i & j). At week 8, the expression level of β-catenin in the HAM + Kaem group exhibited a significant increase compared to the HAM group ($P= 0.027$) (Fig 3j).

Results of Histopathological evaluation

Histopathological examinations conducted at week 4 revealed a significant increase in callus formation and total fracture repair scores in the HAM + Kaem group compared to the control group, with P-values of 0.038 and 0.013, respectively. No significant differences were observed among other histopathological parameters across the groups at week 4 ($P< 0.05$) (Table 4). At week 8, the scores for callus formation, bone union, cortex remodeling, and total fracture repair in the HAM + Kaem group showed significant increases compared to the control group ($P< 0.05$) (Table 4). The total fracture repair score in the Kaem group at week 8 also exhibited a significant increase compared to the control group (P=0.049) (Table 4). Furthermore, the formation of fibrous connective tissue and total tissue response scores at week 8 were significantly higher in the Kaem and HAM + Kaem groups compared to the HAM group ($P< 0.05$). However, no significant differences were observed among the groups for inflammatory cellular infiltration and marrow changes at week 8 (Table 4), (Fig 4 a-h).

Discussion

The results of the present study indicated that the local application of a scaffold composed of a

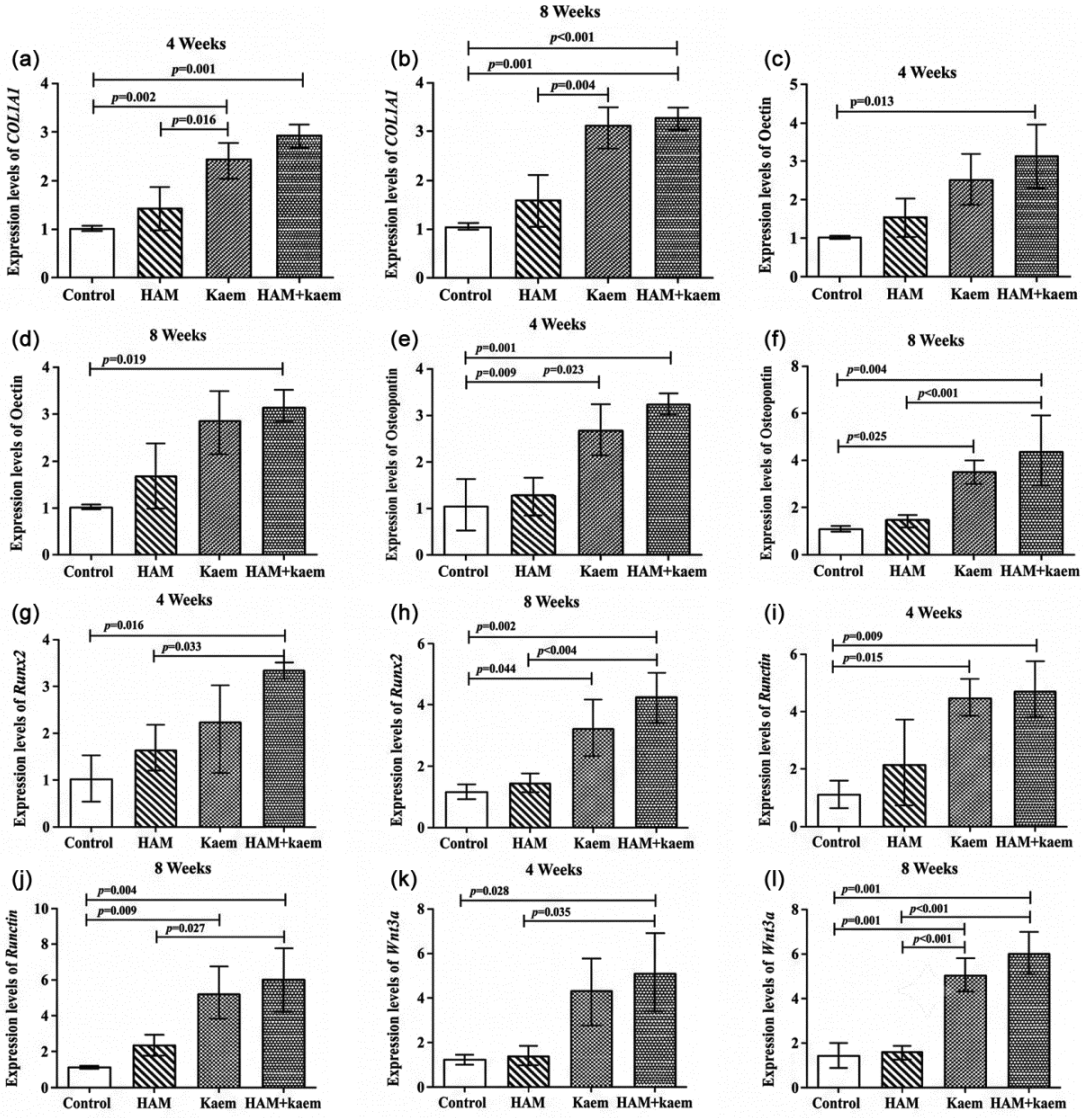


Fig. 3 — Results of the expression levels of the COL1A1, Osterix, Osteopontin, Runx2, β-catenin, and Wnt3a genes at weeks 4 and 8 in the experimental groups. The expression of (a) COL1A1 (in the 4th week); (b) COL1A1 (in the 8th week); (c) Osterix (in the 4th week); (d) Osterix (in the 8th week); (e) Osteopontin (in the 4th week); (f) Osteopontin (in the 8th week); (g) Runx2 (in the 4th week); (h) Runx2 (in the 8th week); (i) β-catenin (in the 4th week); (j) β-catenin (in the 8th week); (k) Wnt3a (in the 4th week); and (l) the Wnt3a (in the 8th week) was used to assess the osteogenesis genes pathway in the experimental groups. The data is displayed as mean ± SD. One-way ANOVA and post hoc Tukey tests were employed. $P< 0.05$ was considered a statistically significant difference. Kaem: Kaempferol, HAM: human amniotic membrane, COL1A1: Collagen Type I Alpha 1 Chain, Wnt3a: Wnt Family Member 3A, Runx2: Runt-Related Transcription Factor 2

combination of HAM and Kaem effectively enhanced the expression of genes involved in the osteogenic pathway and improved bone defects in an experimental model. Specifically, radiological assessments conducted at weeks 4 and 8 revealed a significant increase in the radiological score in the HAM + Kaem group compared to the control group. Furthermore, histopathological evaluations at week 8 demonstrated significant increases in the scores for Callus formation, Bone union, Cortex remodeling, and total Fracture repair in the HAM + Kaem group relative to the control group. Additionally, at week 8, the total fracture repair score in the Kaem group also exhibited a statistically significant increase compared to the control group.

As to the osseous repair, biomaterials functioned as a substrate facilitating the adhesion and proliferation of stem cells. When subjected to various chemical

Table 4 — Comparison of histopathological scores in experimental groups

Variable	Parameters/groups	Score at termination (week 4 of implantation) Control^{-} Mean ± S.D Median (Q1-Q3)	HAM Mean ± S.D Median (Q1-Q3)	Kaem Mean ± S.D Median (Q1-Q3)	HAM + Kaem Mean ± S.D Median (Q1-Q3)	p-value
Fracture repair	Callus formation	0.80±0.45 1 (0.5 - 1)	1.40±0.55 1 (1 – 2)	1.60±0.55 2 (1 – 2)	2.00±0.71* 2 (1.5 – 2.5)	0.048
	Bone union	0.60±0.55 1 (0.0 -1)	0.80±0.45 1 (0.5 – 1)	1.40±0.55 1 (1 – 2)	1.40±0.55 1 (1 – 2)	0.073
	Marrow changes	1.20±0.45 1 (0.5 - 1)	1.20±0.45 1 (1 – 1)	1.40±0.55 1 (1 – 2)	1.40±0.55 1 (1 – 2)	0.824
	Cortex remodeling	0.80±0.45 1 (0.5 - 1)	1.40±0.55 1 (1 – 2)	1.40±0.55 1 (1 – 2)	1.60±0.55 2 (1 – 2)	0.157
	Total score	3.40±0.89 4 (2.5 – 4)	4.80±1.30 4 (4 – 6)	5.80±1.64 5 (4.5 – 7.5)	6.40±0.89* 7 (5.5 – 7)	0.012
Tissue response	Fibrous connective tissue formation	1.40±0.55 1 (1 – 2)	1.80±0.84 2 (1 – 2)	1.00±0.71 1 (0.5 – 1.5)	0.80±0.45 1 (0.5 – 1)	0.133
	Inflammatory cellular infiltration	1.60±0.55 2 (1 – 2)	1.20±0.84 1 (0.5 – 2)	1.00±0.71 1 (0.5 – 1.5)	0.60±0.55 1 (1 – 1)	0.163
	Total score	3.00±0.71 3 (2.5 – 3.5)	3.00±1.58 3 (1.5 – 4.5)	2.00±1.22 2 (1 – 3)	1.40±0.55 1 (1 – 2)	0.072
Variable	Parameters/groups	Score at termination (week 8 of implantation) Control^{-} Mean ± S.D Median (Q1-Q3)	HAM Mean ± S.D Median (Q1-Q3)	Kaem Mean ± S.D Median (Q1-Q3)	HAM + Kaem Mean ± S.D Median (Q1-Q3)	p-value
Fracture repair	Callus formation	1.20±0.45 1 (1 – 1.5)	1.60±0.55 2 (1 – 2)	2.40±0.55 2 (2 – 3)	2.80±0.45* 3 (2.5 – 3)	0.005
	Bone union	1.20±0.45 1 (1 – 1.5)	1.80±0.45 2 (1.5 – 2)	2.40±0.55 2 (2 – 3)	2.80±0.45* 3 (2.5 – 3)	0.005
	Marrow changes	2.20±0.45 2 (2 – 2.5)	2.20±0.45 2 (2 – 2)	2.40±0.55 2 (2 – 3)	2.60±0.55 3 (2 – 3)	0.513
	Cortex remodeling	1.40±0.55 1 (1 – 2)	1.80±0.45 2 (1.5 – 2)	2.60±0.55 3 (2 – 3)	2.80±0.45* 3 (2.5 – 3)	0.008
	Total score	6.00±1.00 6 (5 - 7)	7.40±1.14 7 (6.5 – 8.5)	9.80±1.09* 10 (9 –10.5)	11.00±1.22* 11 (10 – 12)	0.002
Tissue response	Fibrous connective tissue formation	2.20±0.84 2 (1.5 – 3)	2.60±0.55 3 (2 – 3)	0.80±0.45† 1 (0.5 – 1)	0.80±0.45† 1 (0.5 – 1)	0.003
	Inflammatory cellular infiltration	1.20±0.45 1 (1 – 1)	0.80±0.45 1 (0.5 – 1)	0.80±0.45 1 (0.5 – 1)	0.80±0.45 1 (0.5 – 1)	0.414
	Total score	3.40±1.14 3 (2.5 – 4)	3.40±0.55 3 (3 – 4)	1.60±0.89† 2 (1 – 2)	1.60±0.89† 2 (1 – 2)	0.003

* HAM + Kaem vs control or Kaem; †HAM vs Kaem or HAM + Kaem

(Kaem: Kaempferol, HAM: human amniotic membrane, COL1A1: Collagen Type I Alpha 1 Chain, Wnt3a: Wnt Family Member 3A, Runx2: Runt-Related Transcription Factor 2)

compounds, physical stimuli and the surface characteristics of biomaterials, bone stem cells underwent differentiation into osteoblasts, subsequently releasing matrix components that augment calcification and foster the generation of new bone. Simultaneously, growth factors such as BMP-2 are secreted by committed cells, exerting a favorable influence on the recruitment, proliferation, and differentiation of mesenchymal progenitor cells, thus aiding in the *in vivo* formation of bone tissue[30,31]. Empirical investigations have demonstrated that periosteal osteoprogenitor cells translocate to the site of a bone defect, resulting in the generation of new bone in both the peripheral region and on the scaffold surface[30]. Considering the direct relationship between the quantity of osteoblasts and the process of new

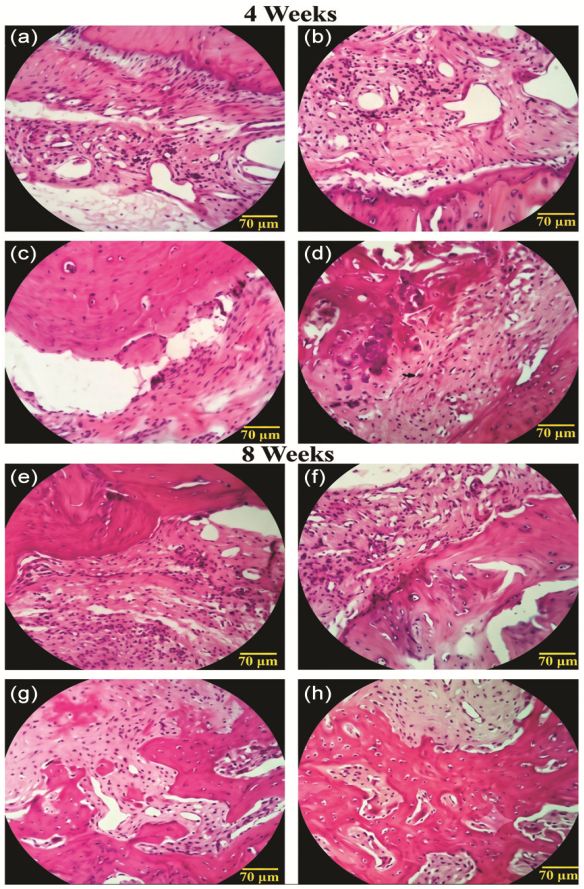


Fig. 4 — Hematoxylin & eosin staining of the rat tibiae defect after covering experimental defects at 4th and 8th weeks. (a & e) Control group, (b & f) HAM group, (C & G) Kaem group, and (d & h) HAM + Kaem group. Histopathological changes observed in the control group at weeks 4 and 8 indicate a lack of organized callus formation and bone tissue, accompanied by a fibrotic tissue response and infiltration of inflammatory cells. The cortical bone has been relatively reconstructed, and the marrow space has been replaced with fibrotic and inflammatory cells. In the HAM group, callus formation was also noted to be irregular, with a widespread tissue response including fibrosis and inflammatory cell infiltration. The cortical bone in this group has shown relative reconstruction. In the Kaem group, organized bone formation and complete repair of the cortical bone were observed, accompanied by a mild tissue response, including fibrosis and infiltration of inflammatory cells. The histopathological changes in the HAM+Kaem group demonstrated organized bone formation and complete repair of the cortical bone with minimal tissue response, including fibrosis and inflammatory cell infiltration. Also, a significant increase in the number of osteoblasts and osteocytes was observed in this group. Kaem: Kaempferol, HAM: human amniotic membrane

bone formation, histopathological assessments indicated that in the HAM + Kaem group, the count of osteoblasts and osteocytes after an eight-week duration was markedly elevated compared to the other groups, thereby underscoring the influence of the Kaem and HAM combination on new bone formation.

Moreover, a study conducted by Sarı *et al*. (2019) demonstrated that HAM positively influenced early fracture healing based on histological scores and measurements of callus diameter at six weeks post-surgery. This effect is attributed to its support for callus formation and maturation, which accelerates bone remodeling[4]. In another study, Mazaki *et al*. reported an increase in the vertebral bone density following Kaem administration[32]. Additionally, Kaem has been shown to create an optimal environment for bone regeneration in bone defects through mechanisms such as stimulating osteoblast activity, reducing oxidative stress and inflammation, enhancing angiogenesis, and inhibiting osteoclast activity. Therefore, the positive effects of the combination of HAM and Kaem on bone defect healing can be attributed to a range of paracrine and cellular properties, as HAM acts as a scaffold while Kaem and other components of HAM enhance cellular proliferation, angiogenesis, and osteogenesis[9,11,26,33,34].

In the present study, the expression levels of the genes Osteopontin, COL1A1, Runx2, Wnt3a, and β-catenin in the Kaem and HAM + Kaem groups showed a significant increase at both the fourth and eighth weeks compared to the control group. Additionally, a significant increase in the expression of the Osterix gene was observed in the HAM + Kaem group relative to the control group at both the fourth and eighth weeks. At week eight, the expression level of the Osterix gene in the Kaem group also demonstrated a significant increase compared to the control group. Furthermore, in the HAM + Kaem group, the expression levels of COL1A1, Runx2, β-catenin, Wnt3a, and Osteopontin also exhibited a significant enhancement compared to the HAM group at week eight.

Laboratory investigations on the influence of Kaem on osteogenesis have elucidated that this compound exerts effects on various specific genes, including ALP, OCN, Osterix, COL1, BMP-2, and Osteopontin, thereby facilitating mineralization in osteoblasts and enhancing calcium nodule deposition[30]. These effects promote the differentiation of MC3T3-E1 pre-osteoblastic cells while simultaneously augmenting their ALP activity and calcification process. Bone formation transpires through either intramembranous or endochondral ossification, during which mesenchymal stem cells undergo differentiation, either directly or indirectly, into osteoblasts, culminating in the creation of a mineralized bone matrix. Kaem possesses the

capacity to modulate various matrix metalloproteinases, thereby directing mesenchymal stem cells towards an osteoblastic lineage through the positive regulation of ALP, Runx-2, Osterix, and OCN, while concurrently diminishing PPAR-γ to inhibit adipogenesis[26,30]. Adhikary et al. demonstrated that the osteogenic potential of Kaem was attributed to its positive regulatory effect on BMP-2, which subsequently led to the proliferation of osteoblasts. They also documented elevated expression levels of Osterix, ALP, Runx-2, OCN, and COL1 in calvarial rat osteoblasts[35].

Laboratory investigations undertaken by Ritu and associates elucidated that Kaem exerted an inhibitory effect on the differentiation of bone marrow-derived mesenchymal stem cells (BMSCs) into adipocytes, concurrently facilitating the differentiation of osteoblasts[36]. In a separate investigation involving the mouse calvarial osteoblast cell line MC3T3, it was observed that Kaem inhibited TNF-α-mediated signaling in osteoblasts, leading to a diminution in the secretion of osteoclastogenic cytokines, specifically interleukin-6 and MCP-1. Furthermore, Kaem obstructed the TNF-α-induced nuclear translocation of NF-κB, a crucial transcriptional regulator of MCP-1. Additionally, Kaem impeded the RANKL-induced differentiation of RAW264.7 cells into osteoclasts by suppressing the expression of c-Fos, a pivotal immediate early oncogene indispensable for the process of osteoclastogenesis[37].

A scholarly investigation conducted by Chiou *et al.* elucidated that administration of 8-prenylkaempferol modulated osteoblast differentiation *via* the BMP-2 signaling cascade, which subsequently resulted in augmented phosphorylation of Smad1/5/8 and the activation of the transcription factor RUNX2, thereby facilitating bone mineralization through the modulation of COL-1, OPN, and ON gene expression[38]. In the current investigation, a statistically significant elevation in the expression levels of the COL1A1 gene and callus score was documented. Empirical research has demonstrated that throughout the process of osseous fracture repair, COL1A1 expression in osteoblasts and mesenchymal stem cells escalated to synthesize the collagen matrix requisite for the development of a reparative callus. An insufficiency in COL1A1 may result in protracted fracture healing; hence, the observed increment in its expression is warranted.

Lai and associates (2022) elucidated that administration of kefir peptides facilitated the fracture healing mechanism and markedly augmented the expression levels of Col1a1, Spp1, Alp, Cox2, and VEGFA in the fractured femora of rats subjected to kefir peptide treatment[39].

In summary, it can be concluded that Kaem accelerates the differentiation of mesenchymal progenitor cells into osteoblasts by activating osteogenic signaling pathways such as BMP-2 and BMP-4. This pathway enhances the phosphorylation of Smad1/5/8, thereby increasing the transcription of osteogenic genes such as Runx2 and Osterix. Additionally, Kaem promotes the accumulation of β-catenin in the nucleus by inhibiting antagonists of the Wnt/β-catenin pathway. This process leads to the activation of genes that are crucial for bone matrix formation. The expression of COL1A1 is regulated by osteogenic factors such as Runx2 and Osterix. The collagen matrix produced from COL1A1 transmits mechanical signals to osteoblasts, which are activated through membrane receptors such as integrins. These signals enhance the differentiation and survival of osteoblasts, and these factors are recognized as key regulators of osteoblast differentiation and bone formation[26,30,33,39]. Therefore, it appears that the combination of Kaem and HAM significantly enhances the strength and speed of bone defect healing.

However, this research had numerous limitations. We employed a single placenta for this experimental investigation. Comparative analyses are essential, in which placentas are sourced from diverse donors to substantiate the reliability of the favorable effects attributed to HAM. While we evaluated radiological, histological, and molecular indicators of fracture healing, we neglected to assess the mechanical integrity of the bone junction. Further biomechanical investigations are warranted in this context. The assessment of osteogenic activity was limited to the mRNA expression levels of the genes, such as COL1A1, Wnt3a, β-catenin, Runx2, osteopontin, and Osterix, without a comparable assessment at the protein level. More research using protein analyses like Western blotting, immunohistochemical staining, or ELISA is required to confirm the activation of osteogenic pathways and better understand the mechanisms by which the kaempferol-loaded dehydrated HAM scaffold promotes bone regeneration, because mRNA expression does not always directly correlate with protein abundance or biological activity due to post-transcriptional and post-translational regulatory processes.

The fundamental mechanisms that govern the facilitation of bone remodeling remain incompletely understood. Consequently, additional clinical and experimental investigations are imperative to clarify the effects of Kaem in conjunction with HAM on the bone healing process.

Conclusion

Critical-sized bone defects, which lack intrinsic healing capabilities, require innovative biomaterial strategies to bridge the gap between structural support and biological function. This study suggests that the synergistic combination of Kaem and HAM may accelerate bone regeneration by enhancing the expression of key osteogenic pathways, including the Wnt/β-catenin signaling pathway, Runx2, osteopontin, and Osterix. Radiographic and histopathological evaluations further showed an improvement in the healing of bone defects. These findings make the combination of Kaem and HAM a promising option for clinical applications in the treatment of non-union fractures and complex orthopedic reconstructions. Although this dual therapy challenges the current paradigm of bone grafting, its long-term efficacy and mechanical details necessitate further exploration through randomized controlled trials and large-scale animal models to fully elucidate its regenerative potential.

Acknowledgement

This study was approved by the Medical Ethics Committee of Xi'an International Medical Center Hospital (ID: GJYX-KY-2024-042). All animal procedures were conducted in accordance with the ARRIVE guidelines

Conflict of interest

All authors declare no conflicts of interest.

References

1 Iaquinta MR, Mazzoni E, Manfrini M, D'Agostino A, Trevisiol L, Nocini R & Trombelli L, Innovative biomaterials for bone regrowth. *Int J Mol Sci*, 20 (2019) 618.

2 Wu Y, Yang H, Zhang X, Liu L, Xu C & Wu K, Exploring YAP1-TEAD interaction in multi-pathway regulation: potential repairing efficacy for bone defect. *Eur Cells Mater*, 52 (2025) 12.

3 Zhang X, Zhang Q, Zhu B & Li R, Wnt/β-catenin-mediated osteogenic repair of osteoporotic defects by dicalcium silicate-activated BMSCs in rats. *Eur Cells Mater*, 54 (2025) 115.

4 Sarı E, Yalçınozan M, Polat B & Özkayalar H, The effects of cryopreserved human amniotic membrane on fracture healing: Animal study. *Acta Orthop Traumatol Turc*, 53 (2019) 485.

5 Li Y, Han X & Ma Z, Research on the mechanical properties of PEEK material artificial bone implants fabricated by high-temperature air-assisted 3D printing. *J Mech Behav Biomed Mater*, 173 (2025) 107207.

6 Pan Y, Liu X, Wang S, Chen L, Li A, Chi Q, Ku X, Xu K & Wang C, Coniferyl Aldehyde in Ginger-Eucommiae Cortex Enhances Osteoarthritis Treatment by Modulating ALDOA and H3K23la Histone Lactylation. *Phytomedicine*, 152 (2026) 157852.

7 Wu M, Zhou Y, He Z, Jiang B & Xu L, Injectable carbon nanotube-reinforced calcium phosphate bone cements with high-strength and improved osteogenesis for bone regeneration. *Colloids Surf B Biointerfaces,* 260 (2025) 115401.

8 Hao X, Jiang B, Wu J, Xiang D, Xiong Z, Li C, Li Z, He S, He S & Li Z, Nanomaterials for bone metastasis. *J Control Release,* 373 (2024) 640.

9 Ghanmi S, Trigui M, Baya W, Ellouz Z, Elfeki A, Charfi S, Fricain JC & Keskes H, The periosteum-like effectof fresh human amniotic membrane on bone regeneration in a rabbit critical-sized defect model. *Bone*, 110 (2018) 392.

10 DiDomenico LA, Orgill DP, Galiano RD, Serena TE, Carter MJ, Kaufman JP, Young NJ & Zelen CM, Aseptically processed placental membrane improves healing of diabetic foot ulcerations: prospective, randomized clinical trial. *Plast Reconstr Surg Glob Open*, 4 (2016) e1095.

11 Tang K, Wu J, Xiong Z, Ji Y, Sun T & Guo X, Human acellular amniotic membrane: a potential osteoinductive biomaterial for bone regeneration. *J Biomater Appl*, 32 (2018) 754.

12 Özgenel GY & Fílíz G, Combined application of human amniotic membrane wrapping and hyaluronic acid injection in epineurectomized rat sciatic nerve. *J Reconstr Microsurg,* 20 (2004) 153.

13 Özgenel GY, The effects of a combination of hyaluronic and amniotic membrane on the formation of peritendinous adhesions after flexor tendon surgery in chickens. *J Bone Joint Surg Br,* 86 (2004) 301.

14 Tejwani S, Kolari RS, Sangwan VS & Rao GN, Role of amniotic membrane graft for ocular chemical and thermal injuries. *Cornea*, 26 (2007) 21.

15 Lee HI, Ha SW & Kim JC, A novel application of amniotic membrane in patients with bullous keratopathy. *J Korean Med Sci,* 21 (2006) 324.

16 Gültekin A, Unal M, Ünlü M & Satoğlu S, Effect of human amniotic fluid and membrane on fracture healing on rat fracture model. *Med J SDU,* 27 (2020) 105.

17 Feng Y, Borrelli M, Reichl S, Schrader S & Geerling G, Review of alternative carrier materials for ocular surface reconstruction. *Curr Eye Res,* 39 (2014) 541.

18 Mohan R, Bajaj A & Gundappa M, Human amnion membrane: potential applications in oral and periodontal field. *J Int Soc Prev Community Dent,* 7 (2017) 15.

19 Huang L, Yagura T & Chen S, Sedative activity of hexane extract of *Keampferia galanga* L. and its active compounds. *J Ethnopharmacol,* 120 (2008) 123.

20 Yang L, Gao Y, Bajpai VK, El-Kammar HA, Simal-Gandara J, Cao H, Cheng KW, Wang M, Arroo RRJ, Zou L, Farag MA & Xiao J, Advance toward isolation, extraction, metabolism and health benefits of kaempferol, a major dietary flavonoid

with future perspectives. *Crit Rev Food Sci Nutr,* 63 (2023) 2773.

21 Devi KP, Malar DS, Nabavi SF, Sureda A, Xiao J, Nabavi SM & Daglia M, Kaempferol and inflammation: From chemistry to medicine. *Pharmacol Res,* 99 (2015) 1.

22 Qin Y, Cui W, Yang X & Tong B, Kaempferol inhibits the growth and metastasis of cholangiocarcinoma *in vitro* and *in vivo. Acta Biochim Biophys Sin*, 48 (2016) 238.

23 Suchal K, Malik S, Khan SI, Malhotra RK, Goyal SN, Bhatia J, Ojha S & Arya DS, Molecular pathways involved in the amelioration of myocardial injury in diabetic rats by kaempferol. *Int J Mol Sci*, 18 (2017) 1001.

24 Zhao J, Wu J, Xu B, Yuan Z, Leng Y, Min J, Lan X & Luo J, Kaempferol promotes bone formation in part *via* the mTOR signaling pathway. *Mol Med Rep,* 20 (2019) 5197.

25 Martiniakova M, Babikova M, Mondockova V, Blahova J, Kovacova V & Omelka R, The role of macronutrients, micronutrients and flavonoid polyphenols in the prevention and treatment of osteoporosis. *Nutrients,* 14 (2022) 523.

26 Wong SK, Chin K-Y & Ima-Nirwana S, The osteoprotective effects of kaempferol: the evidence from *in vivo* and *in vitro* studies. *Drug Des Devel Ther,* 13 (2019) 3497.

27 Zhang Z, Xu W, Zhang Z, Chen X, Jin H, Jiang N & Xu H, The bone-protective benefits of kaempferol combined with metformin by regulation of osteogenesis-angiogenesis coupling in OVX rats. *Biomed Pharmacother*, 173 (2024) 116364.

28 Ghahfarrokhi EK, Meimandi-Parizi A, Oryan A & Ahmadi N, Effects of Combination of bmp7, pfg, and autograft on healing of the experimental critical radial bone defect by induced membrane (masquelet) technique in rabbit. *Arch Bone J Surg,* 9 (2021) 585.

29 Sezgin Sarban M, Senkoylu A, Isikan UE, Petek Korkusuz M & Korkusuz F, Can rhBMP-2 Containing Collagen Sponges Enhance Bone Repair in Ovariectomized Rats. *Clin Orthop Relat Res,* 467 (2009) 3113.

30 Ranjbar FE, Farzad-Mohajeri S, Samani S, Saremi J, Khademi R, Dehghan MM & Azami M, Kaempferol-loaded bioactive glass-based scaffold for bone tissue engineering: in vitro and in vivo evaluation. *Sci Rep,* 13 (2023) 12375.

31 Zheng H, Deng Y, Li B, Huang J, Liu J, Yang Y, Chen Y, Mao L, Li Y, Liu Y, Wang W & Yu H, Xuetongsu attenuates bone destruction in rheumatoid arthritis by suppressing RANKL/RANK/NFATc1 pathway to inhibit osteoclastogenesis and bone resorption. *Bone Joint Res,* 14 (2025) 1016.

32 Mazaki T, Kitajima T, Shiozaki Y, Sato M, Mino M & Yoshida A, In vitro and in vivo enhanced osteogenesis by kaempferol found by a high-throughput assay using human mesenchymal stromal cells, *J Funct Foods*, 6 (2014) 241.

33 Sharma AR & Nam JS, Kaempferol stimulates WNT/β-catenin signaling pathway to induce differentiation of osteoblasts. *J Nutr Biochem,* 74 (2019) 108228.

34 Ramesh P, Jagadeesan R, Sekaran S, Dhanasekaran A & Vimalraj S, Flavonoids: classification, function, and molecular mechanisms involved in bone remodelling. *Front Endocrinol (Lausanne),* 12 (2021) 779638.

35 Adhikary S, Choudhary D, Ahmad N, Karvande A, Kumar A, Banala VT, Mishra PR & Trivedi R, Dietary flavonoid kaempferol inhibits glucocorticoid-induced bone loss by promoting osteoblast survival. *Nutrition*, 53 (2018) 64.

36 Trivedi R, Kumar S, Kumar A, Siddiqui J, Swarnkar G, Gupta V, Kendurker A, Dwivedi AK, Romero JR & Chattopadhyay N, Kaempferol has osteogenic effect in ovariectomized adult Sprague-Dawley rats. *Mol Cell Endocrinol,* 289 (2008) 85.

37 Pang JL, Ricupero DA, Huang S, Fatma N, Singh DP, Romero JR & Chattopadhyay N, Differential activity of kaempferol and quercetin in attenuating tumor necrosis factor receptor family signaling in bone cells. *Biochem Pharmacol*, 71 (2006) 818.

38 Chiou WF, Lee CH, Liao JF & Chen CC, 8-Prenylkaempferol accelerates osteoblast maturation through bone morphogenetic protein-2/p38 pathway to activate Runx2 transcription. *Life Sci*, 88 (2011) 335.

39 Lai JC, Li HP, Chang GRL, Lan YW, Chen YH, Tseng YS, Tu MY, Chen CF, Chen HL & Chen CM, Kefir peptides promote osteogenic differentiation to enhance bone fracture healing in rats. *Life Sci*, 310 (2022) 121090.